

ACCRETION DISK MODELS OF LUMINOUS BLACK HOLES

A.M. Beloborodov¹

¹*Stockholm Observatory, Saltsjöbaden, SE-133 36, Sweden*

ABSTRACT

Models of X-ray production in black-hole sources are reviewed and compared with recent observations. Possible diagnostics of the hot-disk and disk-corona models are discussed in the light of spectral and temporal data. A new model of a small-scale inviscid accretion disk is presented.

INTRODUCTION

About 10% of observed X-ray binaries are thought to harbor black holes (Tanaka & Lewin 1995). In many cases the companion is a low-mass star and the black hole is fed by a gaseous stream pulled out from the companion through the Lagrangian L_1 point. The stream has high angular momentum and a large-scale rotating disk forms around the black hole. In 3 objects (Cyg X-1, LMC X-1, and LMC X-3) the companion is a massive star with a strong wind. The wind-fed accretion flow is quasi-spherical with low angular momentum and can marginally form a small-scale disk.

A standard model was elaborated 3 decades ago for disk accretion onto galactic black holes (GBHs), see review by Pringle (1981). Owing to MHD instabilities the rotating disk is turbulent and viscous (see Balbus & Hawley 1998 for a review). Viscosity dissipates the orbital energy and forces matter to spiral gradually towards the black hole. The bulk of energy is dissipated at a few Schwarzschild radii, $r_g = 2GM/c^2 = 3 \times 10^5 (M/M_\odot)$ cm. The maximum luminosity of the disk is of order of the Eddington limit, $L_{\text{Edd}} = 2\pi r_g m_p c / \sigma_T = 1.3 \times 10^{38} (M/M_\odot)$ erg/s, and the maximum blackbody temperature is

$$kT_{\text{bb}}^{\text{max}} \sim \left(\frac{L_{\text{Edd}}}{\sigma r_g^2} \right)^{1/4} = 7 \left(\frac{M}{M_\odot} \right)^{-1/4} \text{ keV}.$$

Similar accretion flows but of larger scales form around super-massive black holes in AGN, $M \sim 10^8 M_\odot$. According to the $M^{-1/4}$ scaling AGN have $kT_{\text{bb}}^{\text{max}} \sim 70$ eV.

The puzzling property of GBHs and AGN is their hard X-ray emission which sometimes dominates their spectra. It indicates the presence of hot plasmas with temperature $kT \sim 100$ keV and scattering optical depth $\tau_T \sim 1$ near black holes (see reviews by Poutanen 1998, Zdziarski 1999). The plasma may be identified with a hot two-temperature disk (e.g. Shapiro, Lightman & Eardley 1976; Ichimaru 1977) or a corona atop a relatively cold disk (e.g. Bisnovatyi-Kogan & Blinnikov 1977; Galeev, Rosner, & Vaiana 1979), see Beloborodov (1999b, hereafter B99b) for a review. Recently, a new model of a small-scale inviscid disk was developed (Beloborodov & Illarionov 2001, hereafter BI).

OBSERVATIONAL CHARACTERISTICS

The X-ray sources classified as black holes have diverse spectral and temporal properties. Black holes with low-massive companions are normally transient objects and generate outbursts with strong spectral evolution (see King, these proceedings). Persistent high-mass sources may spend most of the time in the hard state dominated by ~ 100 keV emission (Cyg X-1) or in the soft state dominated by ~ 1 keV quasi-blackbody peak (LMC X-1, LMC X-3).

The measured X-ray spectra provide main information on the sources. In both GBHs and AGN the spectrum is well represented as a sum of three components: (1) the quasi-blackbody peak, (2) the intrinsic

power-law emission from the X-ray source, and (3) the reflected/reprocessed X-rays (including the Fe $K\alpha$ line and the Compton reflection bump, see Done, these proceedings). A couple of examples are shown in Fig. 4. The reflector is commonly identified with a (relatively cold, dense) disk. The origin of the hot X-ray source is less clear – different models will be the main subject of this review.

The observed characteristics of the hot source are the photon index of the power law Γ , the position of the spectrum break, and the amplitude of reflection R . The break is almost always at 50 – 200 keV and Γ varies from ~ 2.5 (soft spectra) to ~ 1.5 (hard spectra). The reflection amplitude measures the effective solid angle Ω subtended by the reflector as viewed from the X-ray source, $R = \Omega/2\pi$. In most objects $R < 1$ (see the $R - \Gamma$ diagram in Fig. 2). Recently, a correlation was found between R and Γ in both GBHs and AGN (Zdziarski, Lubiński, & Smith 1999; Gilfanov, Churazov, & Revnivtsev 2000).

Additional information comes from the source variability. Variability is represented by the power density spectrum (PDS) of the fluctuating flux from the source (see Gilfanov, these proceedings). Typically, the power of variability peaks at time-scales $\sim 0.1 - 10$ s. Detailed studies of the PDS of Cyg X-1 and GX 339-4 were recently performed with *RXTE* in different periods of the hard state. In the hardest periods, the variability shifted to longer time-scales (Gilfanov et al. 1999; Revnivtsev et al. 2000).

HOT DISK MODEL

This model postulates the transition from the standard “cold” disk to a hot two-temperature ($T_p \gg T_e$) flow at some radius r_{tr} . The hot flow is a geometrically thick viscous rotating disk that accretes fast and has low density. The mechanism of transition is not well established. One suggestion is that the cold disk may evaporate to a coronal flow atop it (e.g. Różańska & Czerny 2000). The formation of the corona itself, however, depends on complicated MHD processes, and our understanding of these processes is not sufficient to develop a unique transition model. For instance, it is unclear whether the corona stays always “anchored” by the magnetic field to the heavy cold disk or may form an independent accretion flow. Another complicated issue is the heating mechanism and $e - p$ energy distribution in the viscous hot flow. Given these uncertainties, different versions of the hot-disk model can be developed. We will focus here on the phenomenological/observational aspect of the model.

Note that we discuss here *bright* sources (with luminosities $L > 10^{-2}L_{\text{Edd}}$) with substantial radiative efficiency of accretion. Models with small efficiencies (advective flows) designed for low-luminosity sources are reviewed by Marek Abramowicz in these proceedings. An intermediate regime with marginally important advection may apply to the hard-state objects (Esin et al. 1998). It requires: (1) a large viscosity parameter $\alpha \sim 0.3$ and (2) an accretion rate just near the threshold for collapse of the hot flow into a cold disk.

Transition Radius and the X-Ray Spectrum

The parameter r_{tr} is especially important from the observational point of view. The energy released at $r > r_{\text{tr}}$, L_d , emerges as soft radiation according to the standard model (Shakura & Sunyaev 1973). The energy released at $r < r_{\text{tr}}$, L_X , is dissipated in the hot flow that emits X-rays; a fraction of this energy can be stored in the flow and advected into the black hole (or away from it if an outflow forms).

The outer disk illuminates the central hot flow and cools it via Comptonization. For illustration, we will focus here on one version of this model where the outer disk is the main source of soft photons. Alternatively, the photons may be supplied by cold dense clouds embedded in the flow (e.g. Krolik 1998; Zdziarski et al. 1998). Besides, the hot flow itself can generate synchrotron photons (e.g. Esin et al. 1998; Wardziński & Zdziarski 2000) and it becomes especially important if there are non-thermal particles whose emission is not self-absorbed. The observed $R - \Gamma$ correlation, however, suggests that the X-ray reprocessing by the disk dominates the cooling radiation.

The generated spectrum can be evaluated with a toy model of a homogeneous X-ray sphere of radius R_X (Poutanen, Krolik & Ryde 1997; Zdziarski et al. 1999; Gilfanov et al. 2000). Let us fix $R_X = 10r_g = 20GM/c^2$ (the typical radius where the bulk of accretion energy is liberated) and consider r_{tr} as a model parameter. If $r_{\text{tr}} < R_X$, the cold disk enters the X-ray source and L_X decreases. If $r_{\text{tr}} > R_X$, there appears a “gap” between the outer cold disk and the X-ray emitter; then L_X weakly depends on r_{tr} .

The luminosity L_X is partly reprocessed/reflected from the cold disk. The albedo ~ 0.1 for a neutral reflector; then 90% of the X-rays impinging the disk are reprocessed into blackbody soft radiation. The observed blackbody component has luminosity $L_{\text{bb}} = L_d + L_{\text{repr}}$ where L_{repr} is the reprocessed luminosity.

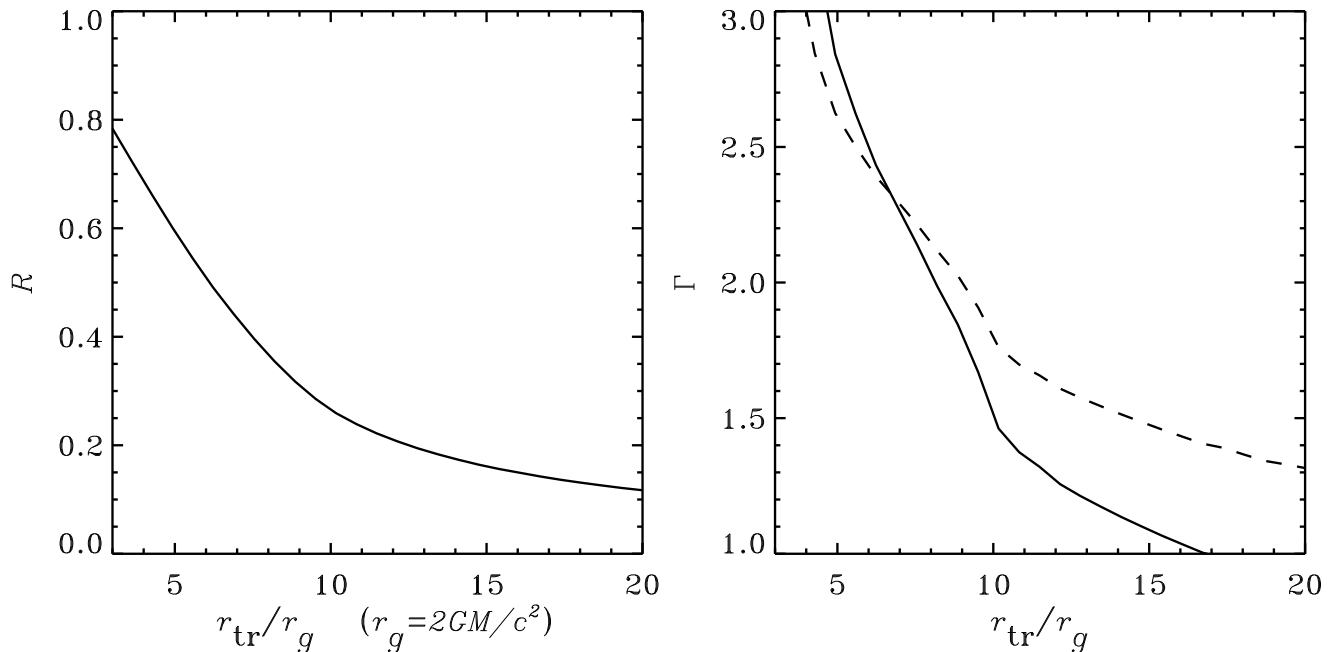


Fig. 1. The dependence of R and Γ on the transition radius. Solid and dashed curves correspond to GBHs ($\delta = 1/6$) and AGN ($\delta = 1/10$) respectively (see eq. 1).

Using the standard Monte-Carlo technique we compute L_{bb} for given accretion rate and r_{tr} , and then find the soft luminosity entering the X-ray sphere, L_s . In a steady state, the Compton amplification factor of the sphere is $A = (L_X + L_s)/L_s$. The spectral index of the Comptonized radiation is related to A (B99b)

$$\Gamma = \frac{7}{3}A^{-\delta}, \quad (1)$$

where $\delta = 1/10$ for AGN and $\delta = 1/6$ for GBHs. The resulting $\Gamma(r_{\text{tr}})$ is shown in Fig. 1. Note that relevant Γ are obtained in a narrow range $5 < r_{\text{tr}}/r_g < 15$. Large r_{tr} are excluded: then a very small fraction of L_{bb} enters the inner X-ray source, leading to photon starvation and too hard spectrum of the source (this conclusion relies, however, on the assumption that the outer disk is the dominant source of soft radiation).

From the simulation we also determine the reflection amplitude $R(r_{\text{tr}})$. We take into account the attenuation of the observed reflection component by scattering in the hot sphere (hereafter R -attenuation). In the calculations the R -attenuation is estimated assuming Thomson optical depth of the sphere $\tau_T = 1$.

Both R and Γ decrease with r_{tr} . The resulting track on the $R - \Gamma$ diagram is shown in Fig. 2 (solid curve). The model predicts low reflection amplitudes throughout the whole range of spectral indexes. Note that the reflector was assumed to be neutral. If the disk is strongly ionized then reflection is further suppressed.

Variability

The energy release can be unsteady in the inner hot flow, leading to variable emission. The shortest time-scale in the disk is the Keplerian period, $t_K \sim 3 \times 10^{-2}(r/10r_g)^{3/2}(M/10M_\odot)$ s. It is also the typical time-scale for MHD instabilities. On longer time-scales the disk emission is averaged over many rotations and the observed variations may be associated with unsteady radial dynamics of the flow. The radial (accretion) time-scale is $t_a \sim (t_K/2\pi\alpha) \sim 0.1(\alpha/0.2)^{-1}$ s (assuming a thick disk with height $H \sim r$), so the hot disk accretes fast compared to typical observed variability.

Modulations may also come from the outer disk. E.g. r_{tr} may decrease on the accretion time-scale of the outer disk, leading to an increase in R and Γ . Accretion is relatively slow in the standard disk and the rate of variations at $r \sim 10r_g$ is consistent with the observed time-scales of maximum variability (see below).

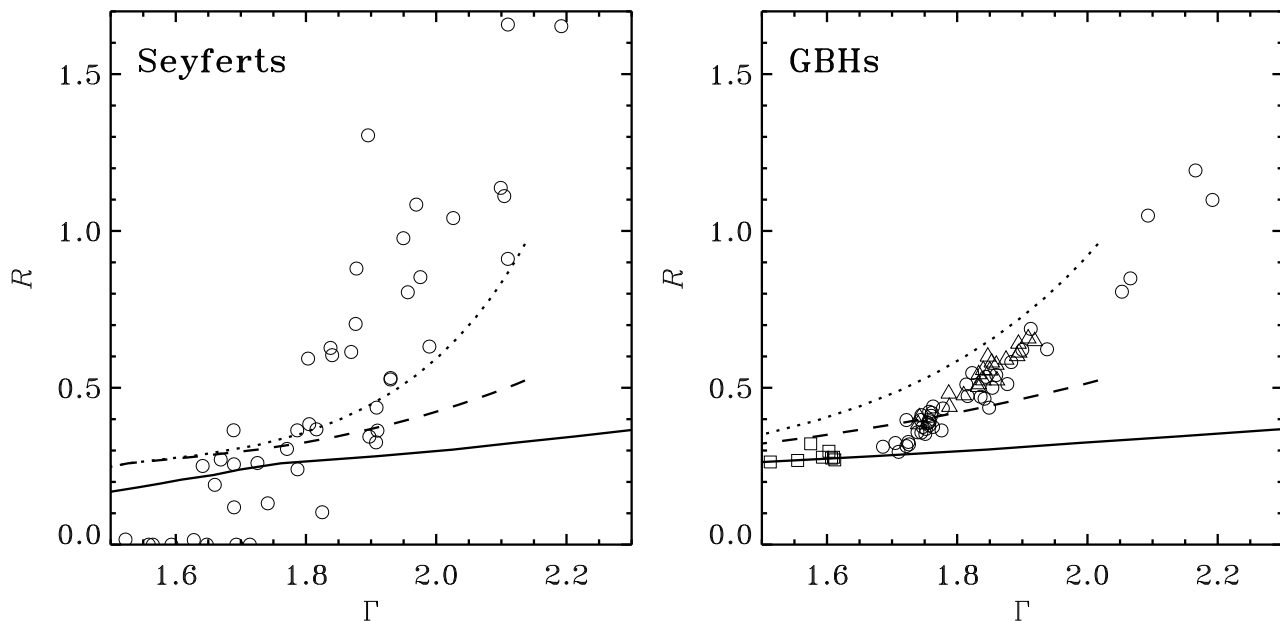


Fig. 2. $R - \Gamma$ diagram (data from Zdziarski et al. 1999, Gilfanov et al. 2000). Symbols show the best-fit values (large errors are not shown here, see Zdziarski et al. 1999). Solid curve shows the model computations for the hot disk. The main cooler of the X-ray source turns out to be the intrinsic radiation of the cold disk rather than reprocessed radiation. To emphasize the importance of intrinsic radiation, we also show the model where only reprocessed radiation cools the X-ray sphere (dashed curve). Dotted curve shows the model where both the intrinsic luminosity of the cold disk and the R -attenuation effect are neglected.

DISK-CORONA MODEL

In this model, the dense thin disk extends down to the marginally stable orbit and the X-ray emission is attributed to its coronal activity. Hot coronae are believed to form as a result of magnetorotational instabilities in the disk and the buoyancy of the generated magnetic field (Tout & Pringle 1992; Miller & Stone 2000). The corona is heated in flare-like events of magnetic dissipation producing the variable X-ray emission. There is no unique model for the coronal activity; like the hot-disk model, the parameters of the putative corona are inferred from observations.

The two main parameters are: (1) the fraction of viscous energy that is released in the corona, f , (the remaining fraction, $1 - f$, is dissipated inside the disk). Observations require f up to $\sim 50\%$ and similar values are suggested by the MHD models. (2) The feedback factor $D = L_s/L$ that is the fraction of the X-ray luminosity that is reprocessed *and* reenters the X-ray source (Haardt & Maraschi 1993; Stern et al. 1995; Poutanen & Svensson 1996). The geometry of the X-ray corona is unknown: it may be e.g. a large cloud covering the whole inner region of the disk or a number of small-scale blobs (flares) with short life-times. From the spectral point of view, the only important parameter of the geometry is the effective feedback D that regulates the temperature of the corona and determines its equilibrium Compton amplification factor,

$$A = \frac{L}{L_s} = \frac{1}{D}. \quad (2)$$

This equation states the energy balance of the corona (here, for simplicity, the intrinsic flux from the disk has been neglected compared to the reprocessed flux; this is the case for intense concentrated flares).

Static Corona with Neutral Reflector

Most of the previous computations of the disk-corona spectra assumed a static corona located atop a neutral reflector (see reviews by Svensson 1996, Poutanen 1998). The model was successfully applied to a number of Seyfert 1s. However, it was found to disagree with observations of black-hole sources in the hard state, e.g. Cyg X-1 (Gierliński et al. 1997). The model never predicts small R simultaneously with hard spectra, in particular $R \sim 0.3$ and $\Gamma \sim 1.6$ observed in Cyg X-1 cannot be reproduced. Furthermore, changes in the coronal geometry produce an anticorrelation between Γ and R (Malzac, Beloborodov, & Poutanen 2001, hereafter MBP). This anticorrelation is opposite to what is observed.

Static Corona with Ionized Reflector

The X-rays from concentrated flares can strongly ionize the upper layers of the disk. In the limit of complete ionization, the disk would resemble a perfect mirror at energies $h\nu < 20$ keV: a power-law incident spectrum is reflected into a power-law without any reflection features and an observer will derive $R = 0$. Ionization substantially reduces the observed amplitude of reflection when the ionization parameter $\xi \gtrsim 10^3$ (e.g. Życki et al. 1994; Ross, Fabian, & Young 1999; Nayakshin, Kazanas, & Kallman 2000).

Approximately, the ionized “skin” of the disk can be represented as a completely ionized layer at a Compton temperature $kT_C \sim 10$ keV atop a neutral reflector. With increasing ionization parameter, the optical depth of the skin τ_s increases and the amplitude of reflection is suppressed. Also the reprocessed radiation is suppressed, leading to a harder spectrum of the corona. The hardness of the spectrum leads to even larger τ_s (Done & Nayakshin 2001).

For illustration consider a slab corona atop optically thick neutral material and a skin τ_s between them. The X-ray flux illuminating the skin, F_i , is mostly reflected after a few scatterings, and a fraction $F_1 \sim (1 + \tau_s)^{-1} F_i$ reaches the neutral material. The neutral material reflects a fraction $a \sim 0.1$ of F_1 and the rest is reprocessed into blackbody radiation. The blackbody component then diffuses out of the skin with a “mirror” inner boundary condition and emerges with flux $\approx F_1$. The reflection component diffuses with an absorbing inner boundary and it gets additionally suppressed by a factor $\sim (1 + \tau_s)^{-1}$. Thus the skin suppresses R as $\sim (1 + \tau_s)^{-2}$ and L_s as $\sim (1 + \tau_s)^{-1}$.

These estimates however do not work for a patchy corona. In that case one needs a 2D model: the disk is strongly ionized beneath the flare and the ionization parameter (and τ_s) will decrease outside the flare. The reflection features (and possibly the bulk of soft radiation) then comes from the less ionized region around the flare, not from beneath it.

Dynamic Corona

The static model is not self-consistent for e^\pm -dominated flares because the created pairs immediately (on Compton time-scale \ll light-crossing time) acquire the equilibrium bulk velocity $\beta = v/c \sim 0.5$ in the anisotropic radiation field (Beloborodov 1999a, hereafter B99a). Besides, an anisotropic energy input of the flare must eject the hot plasma like the ejection in solar flares. The plasma can be ejected away or towards the disk with the preferential direction away from the disk. One can show that bulk acceleration is also efficient for normal $e - p$ plasma: $\beta > 0.1$ in flares with compactness parameters $l > 10^2$ (B99b). Note also that the proton component may be hot, with about virial temperature, and then the plasma is likely to outflow with a virial velocity $\beta > 0.1$.

Mildly relativistic bulk motion in the X-ray source causes X-ray aberration and strongly affects the observed R and Γ . B99a estimated the dependence of R and Γ on β and found that $R \sim 0.3$ and $\Gamma \sim 1.6$ in Cyg X-1 can both be explained with a neutral reflector assuming that the emitting plasma outflows with $\beta \approx 0.3$. Recently, MBP performed exact Monte-Carlo computations of the X-ray spectra produced by dynamic coronae and confirmed the simple analytical model of B99a. In particular, the spectrum of Cyg X-1 was well modeled with $\beta = 0.3$ (see Fig. 4).

Fig. 3 illustrates the effects of bulk motion on the emitted spectra. In the case of $\beta = 0.3$ (plasma moves upwards) the X-rays are beamed away from the disk; as a result the apparent X-ray luminosity is enhanced while the reprocessed and reflected luminosities are reduced. The low feedback leads to a hard spectrum. In the case of $\beta = -0.2$ (plasma moves downwards) the X-rays are beamed towards the disk and the reprocessed and reflected components are enhanced. The high feedback leads to a soft spectrum.

MBP computed the X-ray spectra from hot cylinders with height to radius ratio h/r taken as a parameter. The observed reflection amplitude can be approximated by formula

$$R(\mu) = \frac{(1 - \beta\mu)^3}{(1 + \beta\mu_s)^2} \left\{ \mu_s \left(1 + \frac{\beta\mu_s}{2} \right) + \frac{(1 - \mu_s) [1 + \beta(1 + \mu_s)/2]}{(1 + \beta)^2} e^{-\tau_T(1 - \mu_s)} \right\}, \quad (3)$$

where $\mu = \cos i$, i is the inclination angle of the disk, and the parameter $\mu_s \approx (h/2r)/\sqrt{1 + (h/2r)^2}$ describes the flare geometry. The reflected luminosity is here represented as a sum of two parts: (1) reflected outside the cylinder base, which does not experience any attenuation, and (2) reflected from the base, which is attenuated depending on τ_T . MBP show that formula (3) is in excellent agreement with exact simulations.

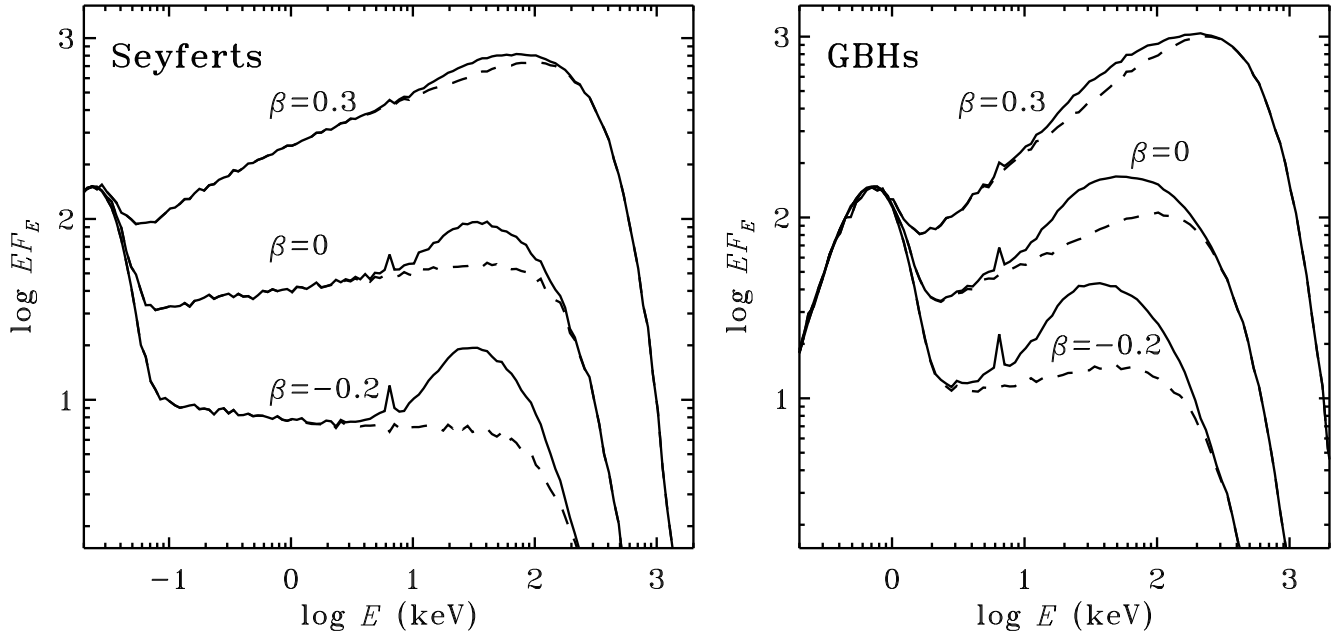


Fig. 3. Effect of bulk motion on the emitted spectra. Here $h/r = 2$, $\tau_T = 3$, and nearly face-on inclination is assumed, $0.9 < \cos i < 1$. (Left) AGN ($kT_{\text{bb}} = 5$ eV). (Right) GBHs ($kT_{\text{bb}} = 150$ eV). (From MBP.)

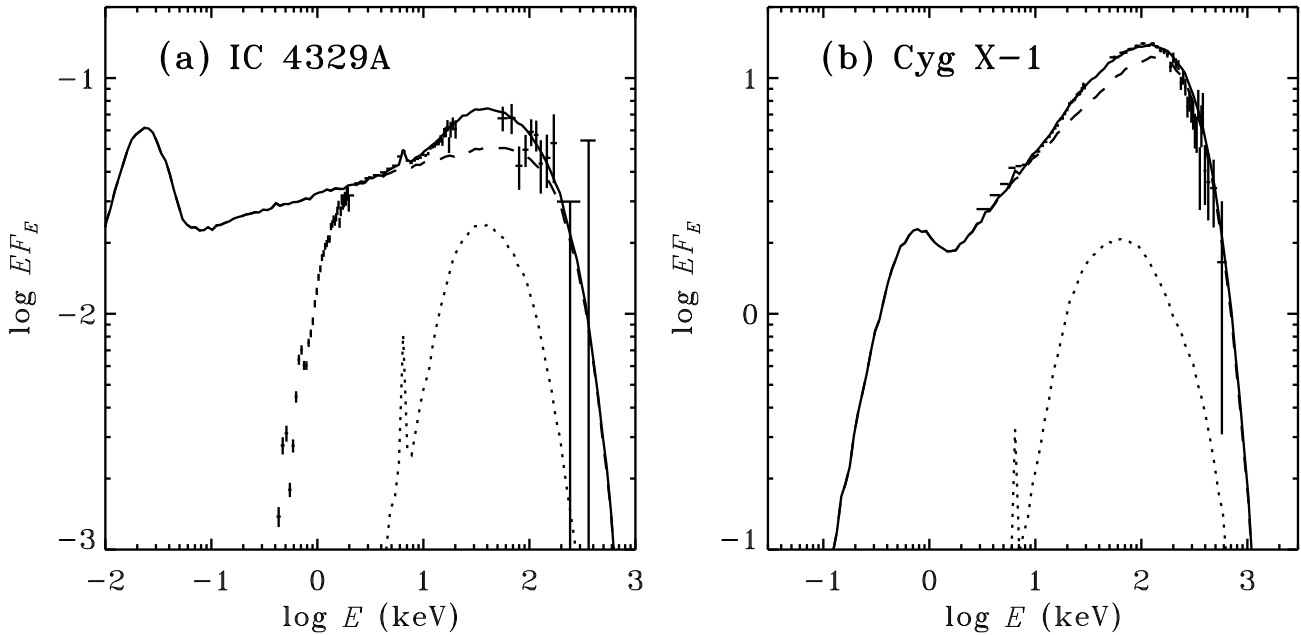


Fig. 4. (Left) Spectrum of the Seyfert 1 galaxy IC4329A (Madejski et al. 1995). Solid curve is the model spectrum for $\tau_T = 3$, $h/r = 2$, $\beta = 0.1$ at inclination $i = 40^\circ$. (Right) Spectrum of Cyg X-1 observed in September 1991 (Gierliński et al. 1997). Solid curve is the model spectrum for $\tau_T = 3$, $h/r = 1.25$, $\beta = 0.3$ at $i = 50^\circ$. In both panels, dotted curves display the reflected components, dashed curves show the intrinsic Comptonized spectra. (From MBP.)

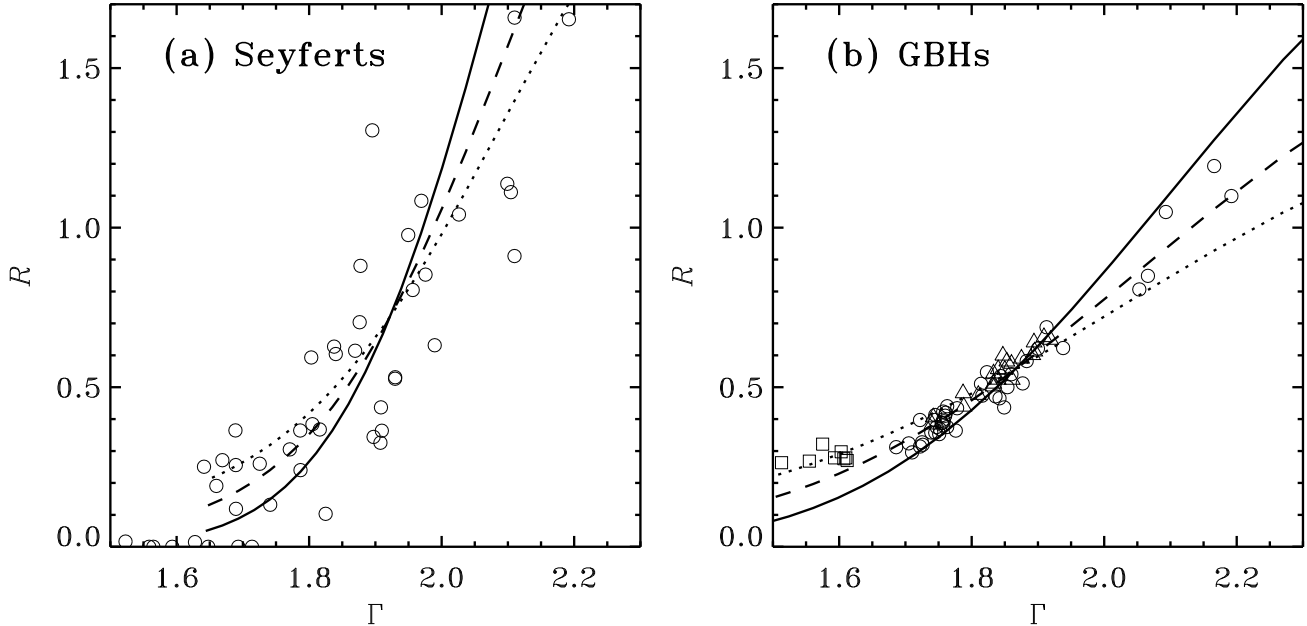


Fig. 5. (Left) R - Γ diagram for Seyfert galaxies; data from Zdziarski et al. (1999). The curves show the dynamic model with $\mu_0 = 0.6$, $\tau_T = 3$, $a = 0.15$ at three different inclinations. (Right) R - Γ diagram for GBHs: Cyg X-1 (circles), GX 339-4 (triangles) and GS 1354-644 (squares); data from Gilfanov et al. (2000). The model curves have $\mu_0 = 0.45$, $\tau_T = 3$, $a = 0.15$. In both panels, solid, dashed, and dotted curves correspond to $i = 30^\circ, 60^\circ$, and 70° , respectively. (From MBP.)

The spectral index of the source, Γ , can be evaluated using relation (1) combined with the formula for the amplification factor (B99a),

$$A = \frac{2\gamma^2(1 + \beta)^2(1 + \beta\mu_s)^2}{(1 - a)(1 - \mu_s)[1 - \beta^2(1 + \mu_s)^2/4]}, \quad (4)$$

where a is the energy-integrated albedo of the disk. Equations (1,3,4) give $R(\beta)$ and $\Gamma(\beta)$ predicted by the dynamic corona model for given μ_s , τ_T , a . With increasing β , R and Γ decrease. The resulting track in the R - Γ diagram is consistent with observations (see Fig. 5).

The important specific prediction of the dynamic corona model is that the scattered soft radiation acquires strong polarization parallel to the disk normal (Beloborodov 1998b), in agreement with optical polarimetric observations of Seyferts (Koratkar & Blaes 1999). Further diagnostics is possible in case the disk emission has a Lyman edge in absorption. Then the observed flux bluewards of the edge should be dominated by the polarized upscattered radiation from the corona. This is consistent with the recently discovered steep rise in polarization bluewards of the Lyman limit (see Beloborodov & Poutanen 1999 and references therein).

Variability

Like the hot-disk model, there is no physical model for variability of coronae (but see Poutanen & Fabian 1999 for a phenomenological model reproducing the observed variability). The life-time of an individual flare is short (probably comparable to Keplerian time, $t_K \sim 10$ ms at $r \sim 10r_g$). The observed variability on longer time-scales can be attributed to changes in the accretion disk dynamics, in particular to variations in the magnetic structure of the disk. A possible time-scale for such variations is the accretion time,

$$t_a \sim \frac{r_g}{\alpha c} \left(\frac{r}{r_g}\right)^{3/2} \left(\frac{r}{H}\right)^2 \sim \frac{r_g}{\dot{m}^2 \alpha c} \left(\frac{r}{r_g}\right)^{7/2} \sim \frac{3}{\dot{m}^2} \left(\frac{M}{10M_\odot}\right) \left(\frac{0.1}{\alpha}\right) \left(\frac{r}{10r_g}\right)^{7/2} \text{ s}, \quad \dot{m} \equiv \frac{\dot{M}}{L_{\text{Edd}} c^2} = \frac{17.5L}{L_{\text{Edd}}}.$$

Here we assumed a non-rotating black hole and a radiation-dominated disk ($L > 10^{-2} L_{\text{Edd}}$). At $r \sim 10r_g$ this time-scale is consistent with the peak in observed PDSs, and smaller radii may be responsible for variability at higher frequencies. The flare ejection velocity probably increases (and R and Γ decrease) at smaller r . This picture may explain the results of Fourier-resolved spectroscopy (Gilfanov et al. 2000).

Transitions between different spectral states may be triggered by variations of e.g. \dot{M} . Observations indicate that when the disk goes to the hard state the intensity of coronal dissipation f increases and an outflow forms. The latter is confirmed by radio observations: radio-jet highly correlates with the hard state (Fender 2000). At the same time, typical time-scales of flux fluctuations increase. It can be naturally explained by deceleration of accretion: the larger f the thinner the cold disk (Svensson & Zdziarski 1994) and t_a grows $\propto (r/H)^2$. If the outflow is not advective, so that the accretion efficiency stays high in the hard state, then the observed flux should be enhanced by beaming at $\dot{M} = \text{const}$. However, the actual behavior of \dot{M} is not known and it possibly decreases in the soft-to-hard transition. This can be tested in high-inclination objects where the observed flux should decrease with decreasing \dot{M} .

SMALL-SCALE INVISCID DISK

Quasi-Spherical Accretion in Bright Sources

In many sources the accretion flow can be quasi-spherical, with low angular momentum l , so that the disk formation is marginal. This is known to be the case in wind-fed X-ray binaries (Illarionov & Sunyaev 1975a,b; Shapiro & Lightman 1976). The net specific angular momentum of the trapped wind matter is $\bar{l}_z \sim (1/4)\Omega R_a^2$ where $R_a = 2GM/w^2 \sim 10^{11}$ cm is the accretion radius, $w \approx 10^8$ cm s $^{-1}$ is the wind velocity, and Ω is the binary angular velocity. From the observed Ω one finds $\bar{l}_z \sim r_g c$ for all the three known X-ray binaries classified as black holes with massive companions (Cyg X-1, LMC X-1, and LMC X-3, see Tanaka & Lewin 1995). The accreting wind matter then inflows quasi-spherically at radii $r_g \ll r < R_a$ with a marginal formation of a small-scale disk at $r \sim r_g$. Similar accretion flows may form around massive black holes in AGN. Among possible gas sources in AGN are star-star collisions and tidal disruption of stars by the black hole (Hills 1975); the accreting gas then likely has modest angular momentum.

Quasi-spherical flows in luminous sources must be Compton cooled and fall freely towards the black hole along ballistic trajectories (Zel'dovich & Shakura 1969). The threshold condition for disk formation reads $l > l_* = 0.75r_g c$: then rotation deflects the trajectories from the radial direction and a ring-like caustic appears in the defocused inflow outside the black hole horizon. Here matter liberates orbital energy in inelastic collision and then proceeds via a thin disk into the black hole. If the inflow has \bar{l}_z comparable to $l_{\text{ms}} = \sqrt{3}r_g c$ (the angular momentum of the marginally stable circular orbit) then the disk differs drastically from its standard counterpart. As we discuss below, such a small-scale disk naturally generates hard X-rays with a break at ~ 100 keV.

The small-scale disk is likely to form in wind-fed sources. Can it also be widespread among other observed sources, for instance AGN? In fact, the dominant majority of objects with quasi-spherical accretion flows may have $l < l_*$ and accrete spherically all the way into the black hole. It should be difficult to observe such objects because of their low luminosity (the efficiency of spherical accretion is probably low). When l exceeds l_* and the disk forms, the luminosity rises dramatically and the black hole “switches on” as an X-ray source. One therefore expects to see preferentially the objects with l above the threshold for disk formation. If the l -distribution of objects falls steeply towards high l , most of the bright sources should be near the threshold, i.e. the regime $\bar{l}_z \sim l_{\text{ms}}$ can be widespread among observed *bright* sources.

Sticky Caustic

For illustration, consider a rotating accretion flow with angular momentum $l(\theta_\infty) = l_0 \sin \theta_\infty$ (i.e. assume solid body rotation at infinity, θ_∞ is polar angle). Free-fall streamlines are symmetric about the equatorial plane and they intersect in the ring-like caustic of radius $r_0 \approx l_0^2/GM$ (Fig. 6). The collisionless shocks enveloping the caustic are pinned to the equatorial plane if the accretion rate is sufficiently high (BI),

$$\dot{m} = \frac{\dot{M}c^2}{L_{\text{Edd}}} > \dot{m}_0 \sim 0.3. \quad (5)$$

For the typical efficiency of the small-scale disk (a few percent) this condition reads $L \gtrsim 10^{-2}L_{\text{Edd}}$. Then the shocked gas forms a thin disk confined by the infall ram pressure. (By contrast, the regime $\dot{m} < \dot{m}_0$ has quasi-spherical shocks that require 2D hydrodynamic simulations, see Igumenshchev, Illarionov, & Abramowicz 1999.) In the regime of pinned shocks, matter falls freely until it reaches the thin shocked disk.

The vertical structure of the disk consists of a cold thin disk and a hot two-temperature layer atop it, where $T_p \gg T_e$. The infalling matter streams from the shock front downwards, passes through the hot layer,

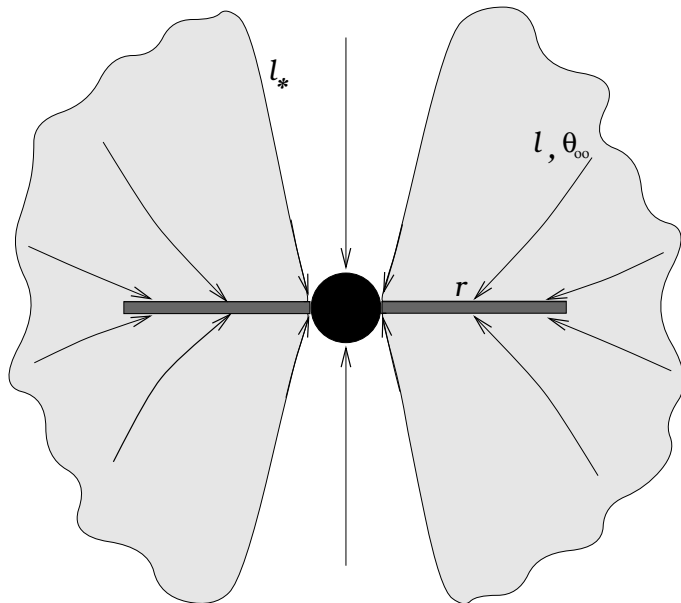


Fig. 6. Schematic picture of disk formation. The shadowed parts of the accretion flow collide outside r_g and form a couple of radiative shocks which sandwich the collision ring. The other part of the flow (at small polar angles where $l < l_*$) is directly swallowed by the black hole with a low radiative efficiency.

cools, and condenses into the cold disk. The electron temperature in the hot layer is found from the balance between Compton cooling and heating by $e - p$ collisions (BI),

$$\frac{kT_e}{m_e c^2} \approx \left(\frac{\ln \Lambda m_e}{\sqrt{2\pi} m_p} \right)^{2/5} \approx 0.1, \quad (6)$$

where $\ln \Lambda \sim 15$ is Coulomb logarithm. Thomson optical depth τ_T of the layer is determined by the time of plasma cooling which yields $\tau_T \approx 1$. The cold disk is geometrically thin and turbulent, with very fast vertical mixing (BI). The disk absorbs the infall and shares its momentum. In this sense, the disk is a “sticky” caustic in the accretion flow and it resembles the accretion line of Bondi & Hoyle (1944).

Inviscid Disk and Its Luminosity

Accretion flows with $\bar{l}_z < 2r_g c$ form disks which can overcome the centrifugal barrier and spiral fast into the black hole without any help of horizontal viscous stresses. Such an “inviscid” disk, however, interacts inelastically with the feeding infall and its streamlines are computed from the laws of momentum and mass conservation (BI), see Fig. 7. The radius of the inviscid disk can be as large as $r_{\max} = 13.6r_g \approx 27GM/c^2$; $r_0 = r_{\max}$ is reached at $l_0 = l_{\text{cr}} \approx 2.62r_g c$. At $l_0 > l_{\text{cr}}$ the centrifugal barrier stops accretion and the steady inviscid regime is not possible. At $l_0 \gg l_{\text{cr}}$ the caustic transforms into the standard viscous accretion disk.

The energy released in the infall-disk collision is radiated. The radial distribution of the luminosity generated by the small-scale inviscid disk is shown in Fig. 7. It peaks at $2r_g$ and a substantial fraction of the luminosity is captured into the black hole. This capture reduces the observed luminosity (the dotted curves in Fig. 7).

X-Ray Spectrum and Variability

The released energy is emitted partly by the hot postshock layer and partly by the cold disk. This structure resembles the disk-corona model. The hot layer is cooled by unsaturated Comptonization producing a power-law spectrum with a break at ~ 100 keV (see eq. 6), in agreement with observations. Γ and R of the spectrum depend on details to be investigated. Note that the postshock layer is likely turbulent and inhomogeneous, and it may resemble a patchy rather than slab corona.

Fluctuations in the angular momentum can cause variations in the size of the small-scale disk ($r \propto l^2$) and even switch the system to a soft spectral state with the standard viscous regime of accretion. This may easily occur in wind-fed X-ray binaries since the trapped l is sensitive to the wind velocity, $l \propto w^4$, and may change substantially. The time-scale for w -variations is not known and can be quite long. The flow is also expected to fluctuate on $t_* \sim 10$ s, the time of accretion from Compton radius (see Illarionov & Beloborodov 2001). The t_* may be associated with the peak in the Fourier spectrum of Cyg X-1.

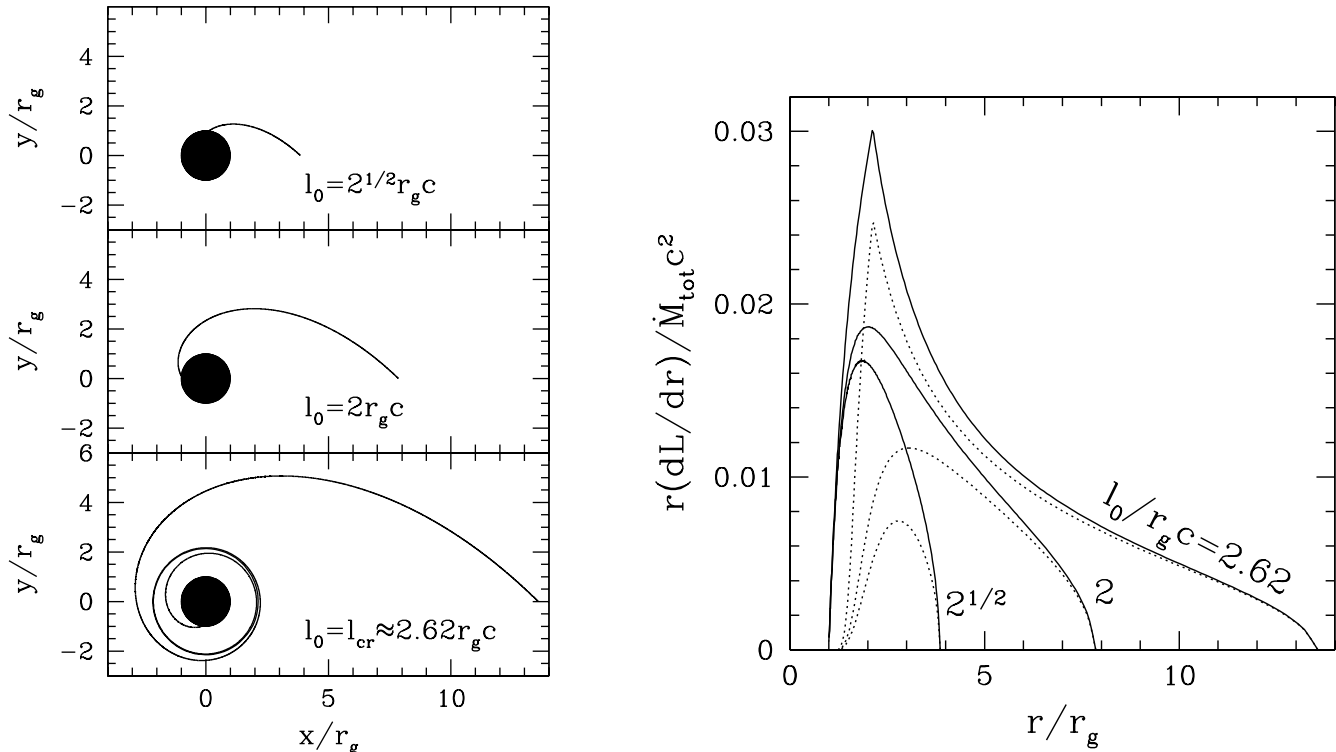


Fig. 7. (*Left*) Streamlines of the disk, from the outer edge into the black hole. The infall has angular momentum $l(\theta_\infty) = l_0 \sin \theta_\infty$. In the critical case (bottom panel) the gas makes infinite number of revolutions at the critical radius $r_{cr} \approx 2r_g$ before it falls into the black hole. (*Right*) Radial distribution of the disk luminosity: solid curves – the released luminosity, dotted curves – the observed luminosity corrected for the capture by the black hole.

Two-component accretion flows (large-scale disk + quasi-spherical inflow) should form in X-ray binaries if the massive companion fills its Roche lobe; similar flows are also possible in AGN. The quasi-spherical component with a maximum angular momentum l_0 will hit the disk inside the radius $r_0 = l_0^2/GM$ and generate power-law X-rays; this interaction may also cause transition to fast inviscid accretion (Beloborodov & Illarionov, in preparation). Outside r_0 , the disk may emit according to the standard model.

SUPER-EDDINGTON DISKS

The pattern of accretion at super-Eddington \dot{M} remains uncertain. It is sensitive to the unknown vertical distribution of heating $q(z)$. Slight increase of q towards upper layers will drive an outflow while homogeneous (or concentrated to the midplane) heating may allow a stable advective inflow. The latter case was studied numerically in the “slim” (vertically integrated) approximation in pseudo-Newtonian (Abramowicz et al. 1988; Chen & Taam 1995) and Kerr (Beloborodov 1998a) gravitational field. 2D simulations (Igumenshchev & Abramowicz 2000) show that different types of flows are possible depending on the viscosity/heating prescription. Future 3D MHD simulations might help to understand the preferred flow pattern at high \dot{M} .

The spectrum of a blackbody pseudo-Newtonian disk was evaluated by Szuszkiewicz, Malkan, & Abramowicz (1996). The blackbody assumption fails at $\alpha > 0.03$: then the thermalization time is longer than the inflow time and the disk overheats up to $\sim 10^9$ K (Beloborodov 1998a).

SUMMARY

The theory of bright black-hole sources is developing and a number of alternative models may account for the data. Three basic possibilities suggested for sub-Eddington accretion are: (1) viscous two-temperature disk, (2) viscous disk with active MHD corona, and (3) small-scale inviscid disk in the inner region of a quasi-spherical inflow. Different regimes of accretion may take place in different objects, depending on the angular momentum of the accreting gas and the accretion rate. All the three models produce Comptonized X-ray spectra with a break at ~ 100 keV. In general, an observed Comptonized spectrum is degenerate, i.e. it is insensitive to the heating mechanism and/or the accretion dynamics. Detailed studies of the spectrum features such as the Fe $K\alpha$ line and the Compton reflection bump might help to break the degeneracy. Also further studies of source variability can provide useful constraints on the models.

REFERENCES

- Abramowicz, M. A., Czerny, B., Lasota, J. P., and E. Szuszkiewicz, Slim Accretion Disks, *ApJ*, **332**, 646-658, 1988.
- Balbus, S. A., and J. F. Hawley, Instability, Turbulence, and Enhanced Transport in Accretion Disks, *Rev. Mod. Phys.*, **70**, 1-53, 1998.
- Beloborodov, A. M., Super-Eddington Accretion Discs around Kerr Black Holes, *MNRAS*, **297**, 739-746, 1998a.
- Beloborodov, A. M., Polarization Change Due to Fast Winds from Accretion Disks, *ApJ*, **496**, 105-108, 1998b.
- Beloborodov, A. M., Plasma Ejection from Magnetic Flares and the X-Ray Spectrum of Cygnus X-1, *ApJ*, **510**, L123-L126, 1999a.
- Beloborodov, A. M., Accretion Disk Models, in High Energy Processes in Accreting Black Holes, eds. J. Poutanen R. Svensson, ASP Conf. Series V. 161, pp. 295-314, Astron. Soc. Pac., San Francisco, 1999b.
- Beloborodov, A. M., and A. F. Illarionov, Small-Scale Inviscid Accretion Disks around Black Holes, *MNRAS*, in press, 2001. (BI)
- Beloborodov, A. M., and J. Poutanen, On the Origin of Polarization near the Lyman Edge in Quasars, *ApJ*, **517**, L77-L80, 1999.
- Bisnovatyi-Kogan, G. S., and S. I. Blinnikov, Disk Accretion onto a Black Hole at Subcritical Luminosity, *A&A*, **59**, 111-125, 1977.
- Bondi, H., and F. Hoyle, On the mechanism of accretion by stars, *MNRAS*, **104**, 273, 1944.
- Done, C., and S. Nayakshin, Observational Signatures of X-Ray Irradiated Accretion Disks, *ApJ*, **546**, 419-428, 2001.
- Esin, A. A., Narayan, R., Cui, W., Grove, J. E., and S.-N. Zhang, Spectral Transitions in Cygnus X-1 and Other Black Hole X-Ray Binaries, *ApJ*, **505**, 854-868, 1998.
- Fender, R. P., Powerful Jets from Black Hole X-Ray Binaries in Low/Hard X-Ray States, *MNRAS*, in press, 2000.
- Galeev, A. A., Rosner, R., and G. S. Vaiana, Structured Coronae of Accretion Disks, *ApJ*, **229**, 318-326, 1979.
- Gierliński, M., Zdziarski, A. A., Done, C., Johnson, W. N., et al., Simultaneous X-Ray and Gamma-Ray Observations of Cyg X-1 in the Hard State by GINGA and OSSE, *MNRAS*, **288**, 958-964, 1997.
- Gilfanov, M., Churazov, E., and M. Revnivtsev, Reflection and Noise in Cygnus X-1, *A&A*, **352**, 182-188, 1999.
- Gilfanov, M., Churazov, E., and M. Revnivtsev, Comptonization, Reflection and Noise in Black Hole Binaries, in 5th CAS/MPG Workshop on High Energy Astrophysics, in press (astro-ph/0002415), 2000.
- Haardt F., and L. Maraschi, X-Ray Spectra From Two-Phase Accretion Disks, *ApJ*, **413**, 507-517, 1993.
- Hills, J. G., Possible Power Source of Seyfert Galaxies and QSOs, *Nature*, **254**, 295-298, 1975.
- Ichimaru, S., Bimodal Behavior of Accretion Disks – Theory and Application to Cygnus X-1 Transitions, *ApJ*, **214**, 840-855, 1977.
- Igumenshchev, I. V., and M. A. Abramowicz, Two-dimensional Models of Hydrodynamical Accretion Flows into Black Holes, *ApJS*, **130**, 463-484, 2000.
- Igumenshchev, I. V., Illarionov, A. F., and M. A. Abramowicz, Hard X-Ray-emitting Black Hole Fed by Accretion of Low Angular Momentum Matter, *ApJ*, **517**, L55-L58, 1999.
- Illarionov, A. F., and A. M. Beloborodov, Free-Fall Accretion and Emitting Caustics in Wind-Fed X-Ray Sources, *MNRAS*, in press, 2001.
- Illarionov, A. F., and R. A. Sunyaev, Why the Number of Galactic X-Ray Stars Is So Small? *A&A*, **39**, 185, 1975a.
- Illarionov, A. F., and R. A. Sunyaev, X-Ray Variability through Accretion by a Black Hole in a Detached Binary System, *Soviet Astron. Lett.*, **1**, 73-74, 1975b.
- Koratkar, A., and O. Blaes, The Ultraviolet and Optical Continuum Emission in Active Galactic Nuclei: The Status of Accretion Disks, *PASP*, **111**, 1-30, 1999.
- Krolik, J. H., A New Equilibrium for Accretion Disks Around Black Holes, *ApJ*, **498**, L13-L16, 1998.
- Madejski, G. M., Zdziarski, A. A., Turner, T. J., Done, C., Mushotzky, R. F., et al., Joint ROSAT-Compton GRO Observations of the X-Ray Bright Seyfert Galaxy IC 4329A, *ApJ*, **438**, 672-679, 1995.

- Malzac, J., Beloborodov, A. M., and J. Poutanen, X-Ray Spectra of Accretion Discs with Dynamic Coronae, *MNRAS*, in press, 2001. (MBP)
- Miller, K. A., and J. M. Stone, The Formation and Structure of a Strongly Magnetized Corona above a Weakly Magnetized Accretion Disk, *ApJ*, **534**, 398-419, 2000.
- Nayakshin, S., Kazanas, D., and T. R. Kallman, Thermal Instability and Photoionized X-Ray Reflection in Accretion Disks, *ApJ*, **537**, 833-852, 2000.
- Poutanen J., Accretion Disc-Corona Models and X/Gamma-Ray Spectra of Accreting Black Holes, in Theory of Black Hole Accretion Discs, eds. M. A. Abramowicz, G. Björnsson G., and J. Pringle, pp. 100-122, Cambridge Univ. Press, Cambridge, 1998.
- Poutanen, J., and A. C. Fabian, Spectral Evolution of Magnetic Flares and Time Lags in Accreting Black Hole Sources, *MNRAS*, **306**, L31-L37, 1999.
- Poutanen, J., and R. Svensson, The Two-Phase Pair Corona Model for Active Galactic Nuclei and X-Ray Binaries: How to Obtain Exact Solutions, *ApJ*, **470**, 249-268, 1996.
- Poutanen, J., Krolik, J. H., and F. Ryde, The Nature of Spectral Transitions in Accreting Black Holes – The Case of Cyg X-1, *MNRAS*, **292**, L21-L25, 1997.
- Pringle, J. E., Accretion Discs in Astrophysics, *ARA&A*, **19**, 137-162, 1981.
- Revnivtsev, M., Gilfanov, M., and E. Churazov, Reflection and Noise in the Low Spectral State of GX 339–4, *A&A*, submitted (astro-ph/9910423), 2000.
- Ross, R. R., Fabian, A. C., and A. J. Young, X-Ray Reflection Spectra From Ionized Slabs, *MNRAS*, **306**, 461-466, 1999.
- Różańska, A., and B. Czerny, Vertical Structure of the Accreting Two-Temperature Corona and the Transition to an ADAF, *A&A*, **360**, 1170-1186, 2000.
- Shakura, N. I., and R. A. Sunyaev, Black Holes in Binary Systems. Observational Appearance, *A&A*, **24**, 337-355, 1973.
- Shapiro, S. L., and A. P. Lightman, Black Holes in X-Ray Binaries - Marginal Existence and Rotation Reversals of Accretion Disks, *ApJ*, **204**, 555-560, 1976.
- Shapiro, S. L., Lightman, A. P., and D. M. Eardley, A Two-Temperature Accretion Disk Model for Cygnus X-1 – Structure and Spectrum, *ApJ*, **204**, 187-199, 1976.
- Stern, B. E., Poutanen, J., Svensson, R., Sikora, M., and M. C. Begelman, On the Geometry of the X-Ray–Emitting Region in Seyfert Galaxies, *ApJ*, **449**, L13-L17, 1995.
- Svensson, R., Models of X-Ray and γ -Ray Emission from Seyfert Galaxies, *A&AS*, **120**, 475-480, 1996.
- Svensson, R., and A. A. Zdziarski, Black Hole Accretion Disks with Coronae, *ApJ*, **436**, 599-606, 1994.
- Szuskiewicz, E., Malkan, M. A., and M. A. Abramowicz, The Observational Appearance of Slim Accretion Disks, *ApJ*, **458**, 474-490, 1996.
- Tanaka, Y., and Lewin, W. H. G., Black-Hole Binaries, in X-ray Binaries, eds. W. H. G. Lewin, J. van Paradijs, and E. P. J. van den Heuvel, pp. 126-174, Cambridge Univ. Press, Cambridge, 1995.
- Tout, C. A., and J. E. Pringle, Accretion Disc Viscosity – A Simple Model for a Magnetic Dynamo, *MNRAS*, **259**, 604-612, 1992.
- Wardziński, G., and A. A. Zdziarski, Thermal Synchrotron Radiation and Its Comptonization in Compact X-ray Sources, *MNRAS*, **314**, 183-198, 2000.
- Zdziarski, A. A., X-Rays and Soft Gamma-Rays from Seyferts, Radio Galaxies, and Black Hole Binaries, in High Energy Processes in Accreting Black Holes, eds. J. Poutanen R. Svensson, ASP Conf. Series V. 161, pp. 16-35, Astron. Soc. Pac., San Francisco, 1999.
- Zdziarski, A. A., Lubiński, P., and D. A. Smith, Correlation Between Compton Reflection and X-Ray Slope in Seyferts and X-Ray Binaries, *MNRAS*, **303**, L11-L15, 1999.
- Zdziarski, A. A., Poutanen, J., Mikołajewska, J., Gierliński, M., Ebisawa, K., and W. N. Johnson, Broad-Band X-Ray/Gamma-Ray Spectra and Binary Parameters of GX 339–4 and Their Astrophysical Implications, *MNRAS*, **301**, 435-450, 1998.
- Zel'dovich, Ya. B., and N. I. Shakura, X-Ray Emission Accompanying the Accretion of Gas by a Neutron Star, *Soviet Astron.*, **13**, 175-183, 1969.
- Życki, P. T., Krolik, J. H., Zdziarski, A. A., and T. R. Kallman, X-Ray Reflection from Photoionized Media in Active Galactic Nuclei, *ApJ*, **437**, 597-610, 1994.